Journal of Sound and Vibration (2002) **256**(5), 955–967
doi:10.1006/jsvi.5028, available online at http://www.idealibrary.com on IDEAL®

SIMPLIFIED DISPERSION RELATIONSHIPS FOR *IN-VACUO* PIPES

W. Variyart and M. J. Brennan

Institute of Sound and Vibration Research, University of Southampton, Southampton SO17 1BJ, England. E-mail: wv@isvr.soton.ac.uk

(*Received* 23 *August* 2001, *and in final form* 10 *December* 2001)

The dispersion characteristics of a pipe offer a way to gain physical insight into its dynamic behaviour. Whilst these can be found in the literature they are generally calculated by numerically solving the characteristic equation. In this paper, a simplified characteristic equation of an *in vacuo* pipe is presented and from this analytical expressions for the wavenumbers for the circumferential modes below the ring frequency are derived. It is shown that before waves cut on and propagate, they change from being decaying standing waves at low frequencies to being nearfield waves. A simplified expression is also determined for the cut on frequencies of the $n \geqslant 2$ circumferential modes. Simulations are presented to validate the results against some established theories of pipe vibration.

1. INTRODUCTION

A convenient way to investigate the dynamic behaviour of a pipe is to examine the characteristics of axial flexural waves in the pipe wall. These are described by axial wavenumbers or wave speeds, which are derived from the characteristic equation of the pipe. In order to explain the dynamic behaviour of the pipe in a simple way, Lin and Morgan [1] used the concept of a rigid tube and an infinitely flexible tube to construct a curve of phase velocity in the axial direction. With this curve, they concluded that all the modes except the first two modes, which are the $n = 0$ and 1 modes where n is the circumferential mode number, have a minimum cut-on frequency corresponding to a natural frequency of a pipe in the circumferential direction and the first two modes exist at all frequencies. A more explicit explanation was provided by Cremer *et al.* [2], in which the phase velocity in the axial direction was calculated from Kennard's shell theory. By comparing this with the phase velocity of a simple structure, they explained the behaviour of the pipe in terms of a bar, a beam and a plate. However, both pieces of work were limited as they considered only real wave types. A complete set of dispersion curves was presented by Fuller and Fahy [3] based on Donnell–Mushtari shell theory. All of the wave types were considered and discussed in their paper. They demonstrated that there are also complex wave types, which combine to give a standing nearfield wave. Nevertheless, the wavenumbers given in their work are complicated and difficult to interpret. In order to provide a simple physical interpretation, Brennan *et al.* [4] employed a complete set of dispersion curves along with Heckl's concept. They discussed the behaviour of individual waves propagating along the shell in terms of flexural beam-like, plate-like bending, longitudinal and shear waves. Recently, Finnveden [5] described the pipe as being equivalent to the model of Timoshenko beam on a Winkler foundation. With this analysis,

0022-460X/02/$35.00

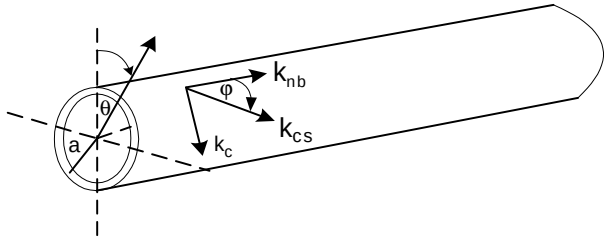

Figure 1. Diagram showing axial, circumferential and helical wavenumbers of an *in vacuo* pipe.

the wavenumber for a propagating wave of the $n \geqslant 1$ modes of the pipe was established in a simple form and it was shown to depend on an equivalent mass and a spring constant for the Winkler foundation. It was clearly illustrated that, before a wave cuts on stiffness dominates the pipe behaviour resulting in a standing nearfield wave, and after it cuts on mass influences the resulting propagating wave.

In this paper, a study of the dispersion characteristics of an *in vacuo* pipe is conducted. To enable greater understanding, the wavenumbers are derived in terms of simple structural waves such as longitudinal, torsional, and flexural waves, wherever possible. However, before the wavenumber analysis can be conducted, the underlying shell theory has to be simplified. This is done using Flügge's shell theory as a basis with some additional assumptions.

2. WAVE MOTION IN AN *IN VACUO* PIPE

For a thin-walled pipe, structural waves propagate in a helical pattern, and can be represented by the wavenumber, k_{cs}, as shown in Figure 1 [6]. This is the vector combination of the wave components in the axial and circumferential directions, and is given by

$$k_{cs}^2 = k_{nb}^2 + k_c^2, \tag{1}$$

where k_{nb} and k_c are the axial and circumferential wavenumbers respectively. The axial wavenumber is thus given by $k_{nb} = \sqrt{k_{cs}^2 - k_c^2}$, which is only real and hence propagating when $k_{cs}^2 \geqslant k_c^2$, otherwise the wave is evanescent. Due to the closure of the pipe in the circumferential direction, the radial displacement of the pipe takes the form of sine or cosine functions of $k_c a\theta$, where $k_c = n/a$; n is the circumferential mode number, a is the radius of a pipe and θ is the azimuthal angle. For the $n = 0$ mode there is only stretching or contracting of the pipe wall, for the $n = 1$ mode, the pipe cross-section is undeformed, and for $n \geqslant 2$ modes the pipe changes in shape as shown in Figure 2. Once the mode shapes are formed around the pipe (i.e., cut on), they propagate independently along the pipe.

With an *in vacuo* pipe, there are eight axial waves that can potentially exist for each mode at any frequency. Four waves travel in the upstream direction and four waves travel in the downstream direction. For the $n \geqslant 2$ modes, below the ring frequency (when the wavelength of a longitudinal wave is equal to the pipe circumference) in the downstream direction, there is a flexural propagating wave ($b = 1$), a nearfield wave ($b = 2$), and a decaying standing wave, which is a combination of two waves ($b = 3$ and 4), which are equal in amplitude but different in phase.

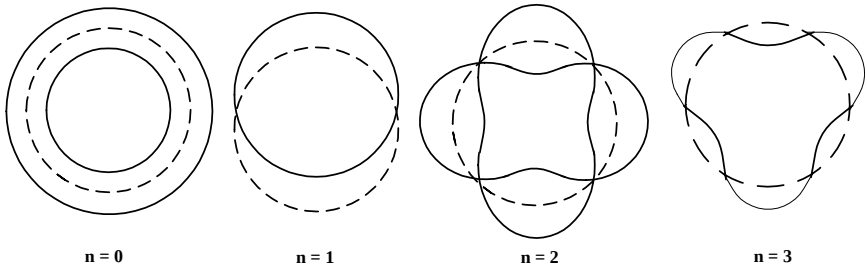

Figure 2. Mode shapes of a pipe.

3. SIMPLIFIED CHARACTERISTIC EQUATION

In this section, a simplified form of the dispersion equation based on Flügge's shell theory is derived. Once this has been established, relatively simple axial wavenumbers are determined for certain conditions. It is assumed that the wall thickness is thin compared to the radius of the pipe, the frequency range of interest is below the ring frequency and the increasing axial flexural wavenumber after the wave cuts on is much greater than the non-dimensional frequency (frequency normalized to the ring frequency). The cylindrical co-ordinate system for a pipe of mid-surface radius a and wall thickness h is shown in Figure 3, where ϕ is a reference angle clockwise from the vertical. The equation of motion of free vibration of the pipe is given by [7, 8]

$$\begin{bmatrix} A_{11} & A_{12} & A_{13} \\ A_{21} & A_{22} & A_{23} \\ A_{31} & A_{32} & A_{33} \end{bmatrix} \begin{bmatrix} u \\ v \\ w \end{bmatrix} = \mathbf{0}, \tag{2}$$

where u, v, w are the axial, tangential, and radial component of the displacements, and

$$A_{11} = \left(\frac{\partial^2}{\partial s^2} + \frac{(1-\nu)}{2}(1+\beta^2)\frac{\partial^2}{\partial \theta^2} - \frac{\rho(1-\nu^2)a^2}{E}\frac{\partial^2}{\partial t^2} \right), \qquad A_{12} = \left(\frac{(1+\nu)}{2}\frac{\partial^2}{\partial s \partial \theta} \right),$$

$$A_{13} = \left(\nu\frac{\partial}{\partial s} - \beta^2\frac{\partial^3}{\partial s^3} + \beta^2\frac{(1-\nu)}{2}\frac{\partial^3}{\partial s \partial \theta^2} \right), \qquad A_{21} = A_{12},$$

$$A_{22} = \left(\frac{(1-\nu)}{2}(1+3\beta^2)\frac{\partial^2}{\partial s^2} + \frac{\partial^2}{\partial \theta^2} - \frac{\rho(1-\nu^2)a^2}{E}\frac{\partial^2}{\partial t^2} \right), \qquad A_{23} = \left(\frac{\partial}{\partial \theta} - \beta^2\frac{(3-\nu)}{2}\frac{\partial^3}{\partial s^2 \partial \theta} \right),$$

$$A_{31} = A_{13}, \qquad A_{32} = A_{23},$$

$$A_{33} = \left(1 + \beta^2\nabla^4 + \beta^2 + 2\beta^2\frac{\partial^2}{\partial \theta^2} + \frac{\rho(1-\nu^2)a^2}{E}\frac{\partial^2}{\partial t^2} \right), \qquad \nabla^4 = \frac{\partial^4}{\partial s^4} + \frac{\partial^4}{\partial \theta^4} + \frac{\partial^4}{\partial s^2 \partial \theta^2}$$

$s = x/a$ being the non-dimensional axial distance along the pipe, $\beta = h/a\sqrt{12}$, and E, ν and ρ are Youngs modulus, the Poisson ratio, and density of the pipe respectively.

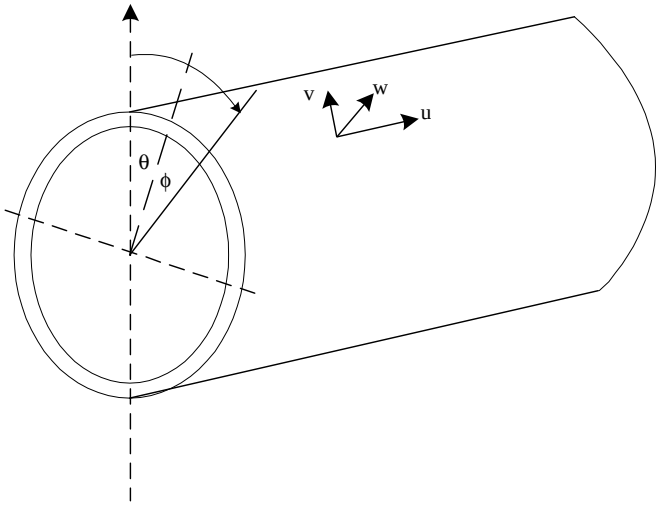

Figure 3. Cylindrical co-ordinate system for a pipe.

The solution of the equation of motion of an *in vacuo* pipe may be written as [9]

$$u(s,\theta,t) = \sum_{n=0}^{\infty}\sum_{b=1}^{8} \bar{\bar{U}}_{nb}\cos[n(\theta-\phi)]e^{j(\hat{k}_{nb}s-\pi/2-\omega t)},$$

$$v(s,\theta,t) = \sum_{n=0}^{\infty}\sum_{b=1}^{8} \bar{\bar{V}}_{nb}\sin[n(\theta-\phi)]e^{j(\hat{k}_{nb}s-\omega t)}, \tag{3a–c}$$

$$w(s,\theta,t) = \sum_{n=0}^{\infty}\sum_{b=1}^{8} \bar{\bar{W}}_{nb}\cos[n(\theta-\phi)]e^{j(\hat{k}_{nb}s-\omega t)},$$

where n is the circumferential mode number, b is the index for the waves, $\hat{k}_{nb}$ is the non-dimensional axial wavenumber (the axial wavenumber multiplied by the radius of the pipe), ω is the angular frequency, and $\bar{\bar{U}}_{nb}$, $\bar{\bar{V}}_{nb}$, $\bar{\bar{W}}_{nb}$ are, respectively, the axial, circumferential, and radial amplitude for the bth wave of the nth mode of the pipe. Substitution of the displacements of equation (3) into equation (2) yields

$$\begin{bmatrix} L_{11} & L_{12} & L_{13} \\ L_{21} & L_{22} & L_{23} \\ L_{31} & L_{32} & L_{33} \end{bmatrix} \begin{bmatrix} \bar{\bar{U}}_{nb} \\ \bar{\bar{V}}_{nb} \\ \bar{\bar{W}}_{nb} \end{bmatrix} = \mathbf{0}, \tag{4}$$

where

$$L_{11} = \hat{k}_{nb}^2 + ((1-\nu)/2)(1+\beta^2)n^2 - \Omega^2, \qquad L_{12} = ((1+\nu)/2)n\hat{k}_{nb},$$

$$L_{13} = \nu\hat{k}_{nb} + \beta^2\hat{k}_{nb}^3 - ((1-\nu)/2)\beta^2 n^2\hat{k}_{nb}, \qquad L_{21} = L_{12},$$

$$L_{22} = ((1-\nu)/2)(1+3\beta^2)\hat{k}_{nb}^2 + n^2 - \Omega^2, \qquad L_{23} = n + ((3-\nu)/2)\beta^2 n\hat{k}_{nb}^2,$$

$$L_{31} = L_{13}, \qquad L_{32} = L_{23},$$

$$L_{33} = 1 + \beta^2 + \beta^2(\hat{k}_{nb}^2 + n^2)^2 - 2\beta^2 n^2 - \Omega^2$$

with $\Omega = \omega/\omega_r$ being the frequency normalized to the ring frequency, where $\omega_r = (1/a)\sqrt{E/\rho(1-\nu^2)}$ is the ring frequency.

The non-dimensional wavenumber, $\hat{k}_{nb}$, of the thin-walled *in vacuo* pipe can be determined by setting the determinant of the matrix in equation (4) to zero, i.e.,

$$|\mathbf{L}| = 0. \tag{5}$$

This can be expanded with terms involving β grouped together, and since for a thin pipe $\beta^2 \ll 1$, then the higher order terms of β (i.e., β^4 and β^6) can be neglected to give

$$\begin{aligned}
&\tfrac{1}{8}\beta^2[\{4(1-\nu)(\hat{k}_{nb}^2+n^2)^2(\hat{k}_{nb}^2+n^2-1)^2+8(1-\nu)^2(\hat{k}_{nb}^4-n^2(n^2-1))\hat{k}_{nb}^2\\
&\qquad+12(1-\nu)^2(1+\nu)\hat{k}_{nb}^4\}\\
&-\Omega^2\{4(3-\nu)(\hat{k}_{nb}^2+n^2)(\hat{k}_{nb}^2+n^2-1)^2+4(1-\nu)(\hat{k}_{nb}^2+n^2)(\hat{k}_{nb}^2+n^2+1)\\
&\qquad+8(1-\nu)(4\hat{k}_{nb}^2+1)\hat{k}_{nb}^2\}]\\
&-\tfrac{1}{2}\Omega^2[(1-\nu)(\hat{k}_{nb}^2+n^2)(\hat{k}_{nb}^2+n^2+1)+2(1-\nu^2)\hat{k}_{nb}^2]+\tfrac{1}{2}(1-\nu)^2(1+\nu)\hat{k}_{nb}^4\\
&\qquad+\tfrac{1}{2}(3-\nu)(\hat{k}_{nb}^2+n^2)\Omega^4+\Omega^4-\Omega^6=0.
\end{aligned} \tag{6}$$

Another assumption that can be made is that $1/\hat{k}_{nb}^2 \gg \beta^2$. This is reasonable for a thin-walled pipe since $\beta^2 \approx 2{\cdot}1\times10^{-4}$ for $h/a = 0{\cdot}05$ while $\hat{k}_{nb}$ increases from zero to about six in the non-dimensional frequency range of zero to one. Since $\hat{k}_{nb} = 2\pi a/\lambda_{nb}$, where λ_{nb} is the axial wavelength of the bth wave of the nth mode, and $\beta = h/\sqrt{12}a$, the assumption can be expressed as, $\lambda_{nb} \gg \pi h/\sqrt{3} \approx 2h$. Physically, this implies that waves with an axial wavelength smaller than about two times of the wall thickness are neglected. In addition, it is assumed that the product of $\beta^2\,\Omega^2$ is very small since the frequency range of interest is below the ring frequency and thus it can also be ignored. After applying these assumptions equation (6) reduces to

$$\begin{aligned}
&\tfrac{1}{2}\beta^2[(1-\nu)(\hat{k}_{nb}^2+n^2)^2(\hat{k}_{nb}^2+n^2-1)^2+2(1-\nu)^2(\hat{k}_{nb}^4-n^2(n^2-1))\hat{k}_{nb}^2]\\
&\quad-\tfrac{1}{2}\Omega^2[(1-\nu)(\hat{k}_{nb}^2+n^2)(\hat{k}_{nb}^2+n^2+1)+2(1-\nu^2)\hat{k}_{nb}^2]+\tfrac{1}{2}(1-\nu)^2(1+\nu)\hat{k}_{nb}^4\\
&\quad+\tfrac{1}{2}(3-\nu)(\hat{k}_{nb}^2+n^2)\Omega^4+\Omega^4-\Omega^6=0.
\end{aligned} \tag{7}$$

Below the ring frequency, this equation can be used to determine the wavenumber–frequency characteristics of a thin-walled pipe for any of the circumferential modes. However, it is still relatively complicated, and can be greatly simplified by making the assumption of $\hat{k}_{nb}^2 \gg \Omega^2$ as used by Heckl [10]. This assumption physically means that wave motion with very long axial wavelengths do not contribute greatly to the overall motion of the pipe. However, this is not true around cut-on frequencies since $\hat{k}_{nb}$ is zero, when Ω has a value between zero and one. A further condition of $\partial\hat{k}_{nb}/\partial\Omega > 1$ just after the wave has cut on is required, which only applies to the $n \geqslant 2$ modes below the ring frequency ($\hat{k}_{nb}$ is proportional to Ω for $n = 0$). Cremer [10] pointed out that this does not result in large errors.

The last three terms containing Ω^4 and Ω^6 in equation (7) including the term $(1-\nu^2)\hat{k}_{nb}^2\Omega^2$ can thus be neglected in comparison with the term $\frac{1}{2}(1-\nu)^2(1+\nu)\hat{k}_{nb}^4$. The term $2(1-\nu)^2\,[\hat{k}_{nb}^4 - n^2(n^2-1)]\,\hat{k}_{nb}^2$ can also be neglected using the previous assumption of $1/\hat{k}_{nb}^2 \gg \beta^2$. Therefore, at frequencies below the ring frequency ($\Omega < 1$), equation (7) becomes for $n \geqslant 2$

$$\begin{aligned}
&\tfrac{1}{2}\beta^2(1-\nu)(\hat{k}_{nb}^2+n^2)^2(\hat{k}_{nb}^2+n^2-1)^2-\tfrac{1}{2}\Omega^2(1-\nu)(\hat{k}_{nb}^2+n^2)(\hat{k}_{nb}^2+n^2+1)\\
&\quad+\tfrac{1}{2}(1-\nu)^2(1+\nu)\hat{k}_{nb}^4=0.
\end{aligned} \tag{8}$$

This can be rearranged to give the relationship between the non-dimensional frequency and the axial wavenumber

$$\Omega^2 = (\beta^2(\hat{k}_{nb}^2 + n^2)^2(\hat{k}_{nb}^2 + n^2 - 1)^2 + (1 - \nu^2)\hat{k}_{nb}^4)/(\hat{k}_{nb}^2 + n^2)(\hat{k}_{nb}^2 + n^2 + 1), \quad n \geqslant 2. \quad (9)$$

The first term on the right side of equation (9) is related to strain energy of the pipe-wall flexure and the second term is related to membrane strain energy [6]. The cut-on frequencies, Ω_{co}, can be determined from equation (9) by setting $\hat{k}_{nb} = 0$, to give

$$\Omega_{co}^2 = \beta^2 n^2 (n^2 - 1)^2/(n^2 + 1). \quad (10)$$

The cut-on frequency given in the above equation is similar to that reported by Finnveden [5], Pavic [11] and Johns and Allwood [12]. It can be further simplified to $\Omega_{co} \approx \beta(n^2 - \frac{3}{2})$, which will underestimate the cut-on frequencies by 6·8% for the $n = 2$ mode, 1·2% for the $n = 3$ mode and less than 0·4% for $n = 4$ modes.

4. APPROXIMATE AXIAL WAVENUMBERS

In this section, the axial wavenumbers for the circumferential modes are derived in terms of the wavenumbers of simple structures such as a bar, a shaft, a beam and a plate. To obtain the wavenumbers, the roots of the characteristic equation (7) are found for the $n = 0$ and 1 modes, and equation (8) for the $n \geqslant 2$ modes, using a similar approach to that taken by Young [13]. Even though the characteristic equation has been simplified, expressions for the wavenumbers remain rather complicated. To gain more physical insight, further simplification is carried out using some additional assumptions, i.e., (a) β^2 can be neglected compared to unity, (b) higher order wavenumbers can be neglected when considering the small wavenumbers such as the longitudinal and torsional wavenumbers for the $n = 0$ mode and *vice versa* [8].

Equations (7) and (8) can be expressed as a polynomial of axial wavenumbers, $\hat{k}_{nb}$, as

$$g_8\hat{k}_{nb}^8 + g_6\hat{k}_{nb}^6 + g_4\hat{k}_{nb}^4 + g_2\hat{k}_{nb}^2 + g_0 = 0, \quad (11)$$

where the g's are coefficients. Solution of this equation leads to the eight wavenumbers. At low frequencies these can be divided into two groups. One group contains the four small wavenumbers, which are the longitudinal and torsional wavenumbers for the $n = 0$ mode, flexural and nearfield wavenumbers for the $n = 1$ mode and the flexural plate-like and nearfield wavenumbers for the $n \geqslant 2$ modes. The other group contains the four large wavenumbers known as standing nearfield wavenumbers. Since they are distinctive, Flügge [8] suggested that the small wavenumbers could readily be determined by neglecting higher orders and the above equation becomes quadratic in $\hat{k}_{nb}^2$

$$g_4\hat{k}_{nb}^4 + g_2\hat{k}_{nb}^2 + g_0 = 0, \quad (12)$$

which gives the following wavenumbers:

$$\hat{k}_{n1}^2, \hat{k}_{n2}^2 = (1/2g_4)\Big[- g_2 \pm \sqrt{g_2^2 - 4g_0g_4}\,\Big]. \quad (13a, b)$$

By ignoring the lower orders of equation (11), the large wavenumbers can also be determined from the resulting quadratic equation in $\hat{k}_{nb}^2$:

$$g_8\hat{k}_{nb}^4 + g_6\hat{k}_{nb}^2 + g_4 = 0, \quad (14)$$

which gives the wavenumbers

$$\hat{k}_{n3}^2, \hat{k}_{n4}^2 = (1/2g_8)\Big[- g_6 \pm \sqrt{g_6^2 - 4g_4g_8}\,\Big]. \quad (15a, b)$$

Since the above method depends up on the distinction between small and large wavenumbers, this method is useful for the first few circumferential modes of the pipe. However, for the higher modes, such a method can still be applied but is valid only just after the waves cut on where the wavenumbers are relatively small.

The polynomial coefficients of axial wavenumbers, $\hat{k}_{nb}$, for the $n = 0$ and 1 modes can be obtained by expanding equation (7) into the polynomial form of equation (11), in which the terms containing $(n^2 - 1)n^2$ are set to zero. They are given by

$$g_8 = ((1 - \nu)/2)\beta^2, \qquad g_6 = (1 - \nu)(2n^2 - \nu)\beta^2, \qquad g_4 = ((1 - \nu)/2)(1 + \beta^2 - \nu^2 - \Omega^2),$$
$$g_2 = -((1 - \nu)/2)[(2n^2 + 1) + 2(1 + \nu)]\Omega^2 + ((3 - \nu)/2)\Omega^4,$$
$$g_0 = \tfrac{1}{2}[(3 - \nu)n^2 - (n^2 + 1)n^2\Omega^2 + 2(1 - \Omega^2)]\Omega^4. \tag{16a–e}$$

4.1. AXIAL WAVENUMBERS OF THE $n = 0$ MODE

By neglecting β^2 in comparison with unity, the coefficients for the $n = 0$ mode given in equation (16) can be written in terms of the non-dimensional longitudinal ($\hat{k}_l$) and torsional ($\hat{k}_s$) wavenumbers normalized to the radius of the pipe (described in Appendix A) as follows:

$$g_8 = ((1 - \nu)/2)\beta^2, \qquad g_6 = -(1 - \nu)\nu\beta^2, \qquad g_4 = ((1 - \nu)(1 - \nu^2)/2)(1 - \hat{k}_l^2),$$
$$g_2 = -((1 - \nu)(1 - \nu^2)/2)[(1 - \hat{k}_l^2)(\hat{k}_l^2 + \hat{k}_s^2) + \nu^2\hat{k}_l^4],$$
$$g_0 = ((1 - \nu)(1 - \nu^2)/2)[1 - (1 - \nu^2)\hat{k}_l^2]\hat{k}_l^2\hat{k}_s^2. \tag{17a–e}$$

Solving for small wavenumbers using equation (13) gives

$$\hat{k}_{01}^2 = \hat{k}_l^2 + \nu^2\hat{k}_l^4/(1 - \hat{k}_l^2), \qquad \hat{k}_{02}^2 = \hat{k}_s^2. \tag{18a, b}$$

Because at low frequencies, $\Omega^2 \ll 1$, the longitudinal wavenumber is small. Hence, the second term in equation (18a) containing a power of 4 can be neglected in comparison with the first term, which gives

$$\hat{k}_{01}^2 = \hat{k}_l^2, \qquad \hat{k}_{02}^2 = \hat{k}_s^2. \tag{19a, b}$$

The large standing nearfield wavenumbers can be found by solving equation (15) to give

$$\hat{k}_{03}^2, \hat{k}_{04}^2 = \nu \pm \sqrt{\nu^2 - (1 - \nu^2)(1 - \hat{k}_l^2)/\beta^2}. \tag{20a, b}$$

At low frequencies, the second term in the square root containing β^2 is much larger than the first term and hence, equation (20a, b) becomes

$$\hat{k}_{03}^2, \hat{k}_{04}^2 = \pm \mathrm{j}\sqrt{(1 - \nu^2)(1 - \hat{k}_l^2)/\beta^2}, \tag{21a, b}$$

where $\mathrm{j} = \sqrt{-1}$.

4.2. AXIAL WAVENUMBERS OF THE $n = 1$ MODE

Using a similar approach to that used for the axial wavenumbers of the $n = 0$ mode, the wavenumbers of the $n = 1$ mode can be found. For this mode, the non-dimensional longitudinal ($\hat{k}_l$), torsional ($\hat{k}_s$) and flexural beam-like ($\hat{k}_b$) wavenumbers (described in Appendix A) are used to represent the behaviour of the pipe.

By substituting $\hat{k}_l$, $\hat{k}_s$ and $\hat{k}_b$ into equation (16) and neglecting β^2 in comparison with unity, the polynomial coefficients for the $n = 1$ mode can be written as follows:

$$g_8 = ((1-\nu)/2)\beta^2, \qquad g_6 = (1-\nu)(2-\nu)\beta^2, \qquad g_4 = ((1-\nu)(1-\nu^2)/2)(1-\hat{k}_l^2),$$
$$g_2 = -((1-\nu)(1-\nu^2)/2)[(1-\hat{k}_l^2)(\hat{k}_l^2+\hat{k}_s^2)+\nu^2\hat{k}_l^4+\hat{k}_b^4],$$
$$g_0 = ((1-\nu)(1-\nu^2)/2)[\{1-(1-\nu^2)\hat{k}_l^2\}\hat{k}_l^2\hat{k}_s^2+\{\hat{k}_s^2+(1-\nu^2)\hat{k}_l^2\}\hat{k}_l^2-\hat{k}_b^4]. \quad (22a\text{–}e)$$

The small wavenumbers of the $n = 1$ mode are obtained by solving equation (13) to give

$$\hat{k}_{11}^2, \hat{k}_{12}^2 = \{[(1-\hat{k}_l^2)(\hat{k}_l^2+\hat{k}_s^2)+\nu^2\hat{k}_l^4+\hat{k}_b^4]$$
$$\pm\sqrt{[(1-\hat{k}_l^2)(\hat{k}_l^2-\hat{k}_s^2)+\nu^2\hat{k}_l^4]^2+4\hat{k}_b^4-(1-\nu^2)\hat{k}_b^8}\}/2(1-\hat{k}_l^2). \quad (23a, b)$$

This can be compared with the wavenumbers for a Timoshenko beam (k_t) given by [4]

$$k_t^2 = \tfrac{1}{2}[k_{tl}^2+k_{ts}^2/\kappa_t] \pm \tfrac{1}{2}\sqrt{[k_{tl}^2-k_{ts}^2/\kappa_t]+4k_{tb}^4}, \quad (23c, d)$$

where k_{tl}, k_{ts}, k_{tb} are the longitudinal, torsional and flexural beam-like wavenumbers of a beam, and κ_t is Timoshenkos shear coefficient. At relatively low frequencies ($\Omega < 0{\cdot}5$) higher order terms such as $\hat{k}_l^4$ and $\hat{k}_b^8$ can be neglected, and $\hat{k}_l^2$ can be ignored in comparison with unity so equation (23a, b) becomes

$$\hat{k}_{11}^2, \hat{k}_{12}^2 = \tfrac{1}{2}[\hat{k}_l^2+\hat{k}_s^2] \pm \tfrac{1}{2}\sqrt{[\hat{k}_l^2-\hat{k}_s^2]+4\hat{k}_b^4}. \quad (24)$$

Thus, the behaviour of the $n = 1$ mode of the pipe is very similar to a Timoshenko beam in this frequency range. At very low frequencies when $\Omega < 0{\cdot}1$, $\hat{k}_l^2$, $\hat{k}_s^2$ and $\hat{k}_b^4$ are much less than unity and their higher order terms can be ignored. The wavenumbers are then given by

$$\hat{k}_{11}^2, \hat{k}_{12}^2 = \pm\hat{k}_b^2. \quad (25a, b)$$

Thus, at very low frequencies, the $n = 1$ mode of a pipe behaves like an Euler–Bernoulli beam. The large wavenumbers of the $n = 1$ mode can also be determined by solving equation (15) to give

$$\hat{k}_{13}^2, \hat{k}_{14}^2 = -(2-\nu) \pm \sqrt{(2-\nu)^2-(1-\nu^2)(1-\hat{k}_l^2)/\beta^2}. \quad (26a, b)$$

Again, at low frequencies the second term in the square root containing β^2 is much larger than the first term and therefore, equation (26) becomes

$$\hat{k}_{13}^2, \hat{k}_{14}^2 = \pm \mathrm{j}\sqrt{[1-\nu^2)(1-\hat{k}_l^2)/\beta^2}, \quad (27a, b)$$

which are the same as the wavenumbers obtained for the $n = 0$ mode.

4.3. AXIAL WAVENUMBERS OF THE $n \geqslant 2$ MODES

After the waves for the $n \geqslant 2$ modes cut on, the flexural wavenumbers increase rapidly with increasing frequency. The standing nearfield wavenumbers obtained by the method discussed above are limited to low frequencies where there are large differences between them. To allow the method to be used at higher frequencies equation (8) is rewritten with the assumption of $\hat{k}_{nb}^2 + n^2 \gg 1$, to give

$$\beta^2\tau^4 + (1-\nu^2-\Omega^2)\tau^2 - 2(1-\nu^2)n^2\tau + (1-\nu^2)n^4 = 0, \quad (28)$$

where $\tau = \hat{k}_{nb}^2 + n^2$. Neglecting the last term of equation (28) gives

$$\beta^2\tau^3 + (1-\nu^2-\Omega^2)\tau - 2(1-\nu^2)n^2 = 0, \quad (29)$$

from which the wavenumbers of the standing nearfield waves can be determined. The solution of equation (29) is

$$\tau_{n3,n4} = \tfrac{1}{6}[-(3z^{1/3} - (1 - v^2 - \Omega^2)/\beta^2 z^{1/3}) \pm \mathrm{j}\sqrt{3}(3z^{1/3} + (1 - v^2 - \Omega^2)/\beta^2 z^{1/3})], \quad (30)$$

where $z = ((1 - v^2)/\beta^2)[1 + \sqrt{1 + (1 - v^2 - \Omega^2)^3/27(1 - v^2)^2\beta^2 n^4}]n^2$.

Hence, the standing nearfield wavenumbers are given by

$$\hat{k}^2_{n3,n4} = -n^2 + \tfrac{1}{6}[-(3z^{1/3} - (1 - v^2 - \Omega^2)/\beta^2 z^{1/3}) \pm \mathrm{j}\sqrt{3}(3z^{1/3} + (1 - v^2 - \Omega^2)/\beta^2 z^{1/3})]. \quad (31)$$

Because the nearfield wavenumber is small compared with the others it can still be determined using a quadratic equation. By expressing equation (8) in the polynomial form of equation (11), the polynomial coefficients for the $n \geqslant 2$ modes can be written in terms of the cut-on frequency (Ω_{co}) and are given by

$$g_8 = \beta^2, \qquad g_6 = 2\beta^2(2n^2 - 1),$$
$$g_4 = 1 + \beta^2 - v^2 - \Omega^2 + 6\Omega^2_{co}((n^2 + 1)/(n^2 - 1)) \cong 1 - v^2 - \Omega^2 + 6\Omega^2_{co},$$
$$g_2 = 2\Omega^2_{co}(2n^2 - 1)((n^2 + 1)/(n^2 - 1)) - \Omega^2(2n^2 + 1) \cong -2n^2(\Omega^2 - 2\Omega^2_{co}),$$
$$g_0 = n^2(n^2 + 1)(\Omega^2_{co} - \Omega^2) \cong -n^4(\Omega^2 - \Omega^2_{co}). \quad (32a\text{–}e)$$

From these, the nearfield wavenumber, $\hat{k}_{n2}$, is found using equation (13) and is

$$\hat{k}^2_{n2} = n^2\left[(\Omega^2 - 2\Omega^2_{co}) - \sqrt{(1 - v^2 + 3\Omega^2_{co})(\Omega^2 - \Omega^2_{co}) + \Omega^4_{co}}\right]/(1 - v^2 - \Omega^2 + 6\Omega^2_{co}). \quad (33)$$

To determine $\hat{k}_{n1}$, equation (11) is rewritten in the form of

$$g_8(\hat{k}^2_{nb} - \hat{k}^2_{n1})(\hat{k}^2_{nb} - \hat{k}^2_{n2})(\hat{k}^2_{nb} - \hat{k}^2_{n3})(\hat{k}^2_{nb} - \hat{k}^2_{n4}) = 0. \quad (34)$$

Arranging equation (34) in terms of a polynomial of axial wavenumbers, $\hat{k}_{nb}$, gives

$$g_8\hat{k}^2_{nb} - g_8(\hat{k}^2_{n1} + \hat{k}^2_{n2} + \hat{k}^2_{n3} + \hat{k}^2_{n4})\hat{k}^6_{nb}$$
$$+ g_8(\hat{k}^2_{n1}\hat{k}^2_{n2} + \hat{k}^2_{n1}\hat{k}^2_{n3} + \hat{k}^2_{n1}\hat{k}^2_{n4} + \hat{k}^2_{n2}\hat{k}^2_{n3} + \hat{k}^2_{n2}\hat{k}^2_{n4} + \hat{k}^2_{n3}\hat{k}^2_{n4})\hat{k}^4_{nb}$$
$$- g_8(\hat{k}^2_{n1}\hat{k}^2_{n2}\hat{k}^2_{n3} + \hat{k}^2_{n1}\hat{k}^2_{n2}\hat{k}^2_{n4} + \hat{k}^2_{n1}\hat{k}^2_{n3}\hat{k}^2_{n4} + \hat{k}^2_{n2}\hat{k}^2_{n3}\hat{k}^2_{n4})\hat{k}^2_{nb} + g_8\hat{k}^2_{n1}\hat{k}^2_{n2}\hat{k}^2_{n3}\hat{k}^2_{n4} = 0. \quad (35)$$

Following the method suggested by Kreyszig [14], the solution of the flexural wavenumber can be found by comparing the last term in the above equation with the last term in equation (11) to give

$$\hat{k}^2_{n1} = g_0/g_8\hat{k}^2_{n2}\hat{k}^2_{n3}\hat{k}^2_{n4} = \left(-g_2 + \sqrt{g_2^2 - 4g_0g_4}\right)/2g_8\hat{k}^2_{n3}\hat{k}^2_{n4}. \quad (36)$$

Substituting for the polynomial coefficients yields the following expression:

$$\hat{k}^2_{n1} = n^2[(\Omega^2 - 2\Omega^2_{co}) + \sqrt{(1 - v^2 + 3\Omega^2_{co})(\Omega^2 - \Omega^2_{co}) + \Omega^4_{co}}]/\beta^2\hat{k}^2_{n3}\hat{k}^2_{n4}. \quad (37)$$

As previously mentioned, the quadratic method can be used to determine $\hat{k}_{n1}$ and $\hat{k}_{n2}$ when they are relatively small in comparison with the standing nearfield wavenumbers, $\hat{k}_{n3}$ and $\hat{k}_{n4}$. This implies that at very low frequencies, $\beta^2\hat{k}^2_{n3}\hat{k}^2_{n4} \cong 1 - v^2 - \Omega^2 + 6\Omega^2_{co}$. From equations (33) and (37), when $\Omega \ll \Omega_{co}$, $\hat{k}_{n1}$ and $\hat{k}_{n2}$ are standing near fields and can be approximately given by

$$\hat{k}^2_{n1},\ \hat{k}^2_{n2} = n^2[-2\Omega^2_{co} \pm \mathrm{j}\sqrt{(1 - v^2 + 3\Omega^2_{co})\Omega^2_{co}}]/\beta^2\hat{k}^2_{n3}\hat{k}^2_{n4}. \quad (38)$$

TABLE 1

PVC pipe data

E (N/m^2)	ρ (kg/m^3)	v	a (mm)	h (mm)
$3{\cdot}974 \times 10^9$	1460	0·33	33·2	2·2

At Ω around Ω_{co}, the equations can be rewritten as

$$\hat{k}_{n1}^2 = n^2(\Omega^2 - \Omega_{co}^2)/\beta^2\hat{k}_{n3}^2\hat{k}_{n4}^2, \qquad \hat{k}_{n2}^2 = n^2(\Omega^2 - 3\Omega_{co}^2)/\beta^2\hat{k}_{n3}^2\hat{k}_{n4}^2. \tag{39}$$

To determine the frequency at which the $\hat{k}_{n1}$ and $\hat{k}_{n2}$ waves change from standing nearfield waves to nearfield waves the square root term in equations (33) and (37) is set equal to zero to give

$$\Omega = \Omega_{co}\sqrt{(1 - v^2 + 2\Omega_{co}^2)/(1 - v^2 + 3\Omega_{co}^2)}. \tag{40}$$

The frequency interval (Δ) when $\hat{k}_{n1}$ behaves as a nearfield wave is given by

$$\Delta = \Omega_{co} - \Omega = \Omega_{co}\left[1 - \sqrt{1 - \frac{\Omega_{co}^2}{1 - v^2 + 3\Omega_{co}^2}}\right] \cong \frac{\Omega_{co}^3}{2(1 - v^2 + 3\Omega_{co}^2)}. \tag{41}$$

Equation (41) shows that the frequency interval increases with higher circumferential modes of the pipe because of the increasing cut-on frequency, which is demonstrated graphically later in the paper.

5. NUMERICAL EVALUATION OF THE SIMPLIFIED DISPERSION CHARACTERISTICS

A set of dispersion curves from the simplified model developed in the previous sections is compared with those obtained from the shell theories developed by Brevart and Fuller [15], Kennard [16] and Flügge. The properties of the pipe used in the comparison are given in Table 1. To verify the model, simulations were carried out for each mode number. This simplified model is calculated from equations (18) and (20) for the $n = 0$ mode, equations (23a, b) and (26) for the $n = 1$ mode, and equations (31), (33) and (37) for the $n \geqslant 2$ modes. The simulations are shown in Figure 4. It can be seen that Kennard's and Flügge's shell theories give a similar result. There are slight differences at the cut-on frequency for the higher modes due to the different assumptions in both theories.

The discussion for the dispersion curves produced by the simplified model is separated into three groups, breathing ($n = 0$), bending ($n = 1$), and circumferential ($n \geqslant 2$) modes. The positive real and imaginary parts of the non-dimensional wavenumbers, $b = 1, 2, 3$ and 4, are, respectively, presented in the upper and lower parts of the graphs in Figure 4. For the $n = 0$ mode, the model is consistent with Kennard's and shell theory up to about $\Omega = 0{\cdot}9$ before the longitudinal wavenumber ($\hat{k}_l$) reaches unity leading to the singularity of the term $v^2\hat{k}_l^4/(1 - \hat{k}_l^2)$ (equation (18)) resulting in $\hat{k}_{01}$ becoming infinite. When $\hat{k}_l^2 < 1$, this term is small so that the wavenumber $\hat{k}_{01}$ can be approximated by $\hat{k}_l$. The other wavenumbers, $\hat{k}_{02}$ represented by the torsional wave $\hat{k}_s$ and the standing nearfield waves $\hat{k}_{03}$, $\hat{k}_{04}$ are in good agreement with both referenced theories up to the ring frequency. Both $\hat{k}_{03}$, $\hat{k}_{04}$ characterized by a complex wavenumber are equal in magnitude but opposite in phase and are thus standing near field waves whose amplitudes rapidly decay with increasing distance from their source. It can be seen that close to the ring frequency ($\Omega > 0{\cdot}8$), the real

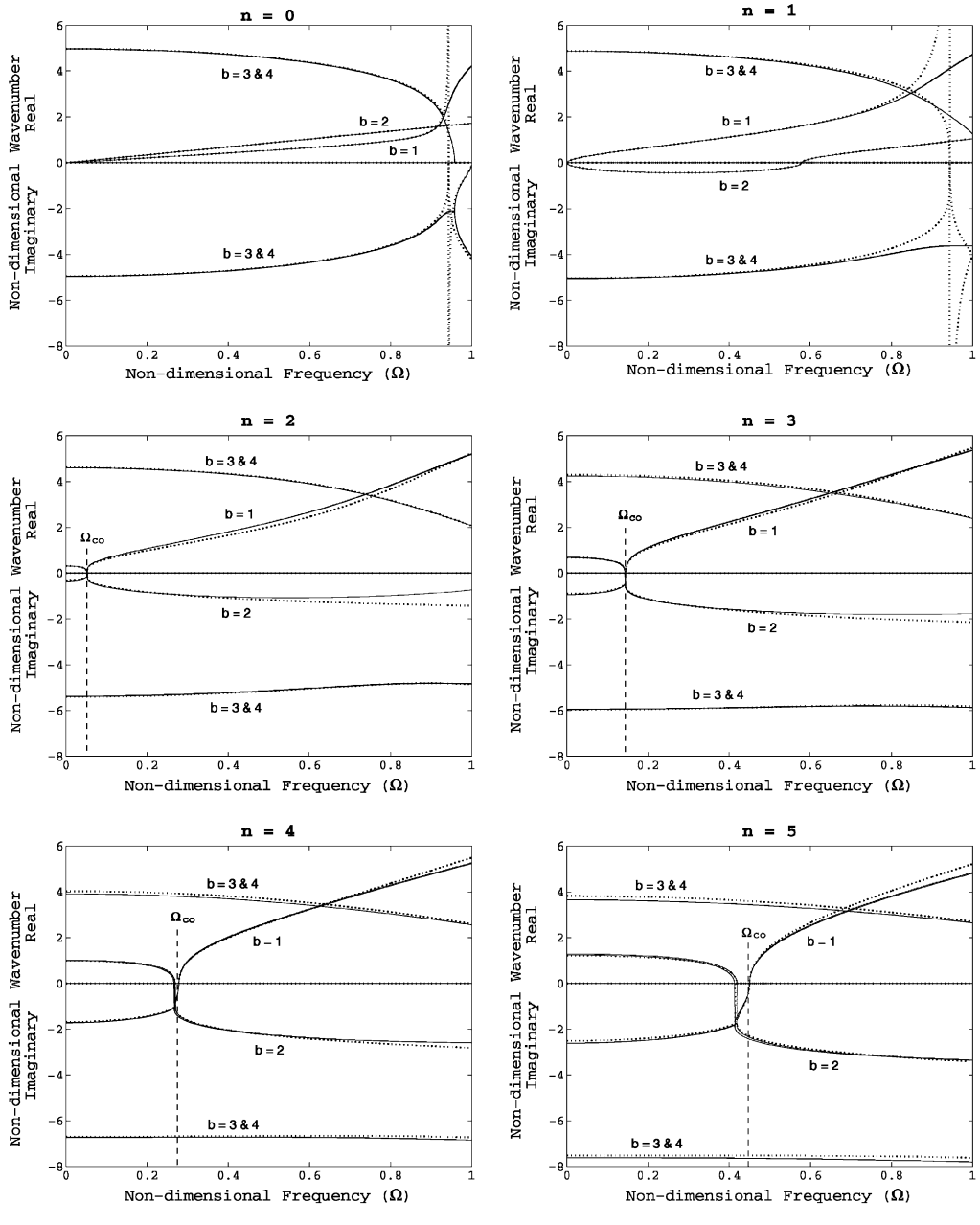

Figure 4. Dispersion curve of the mode number (a) $n = 0$ to (f) $n = 5$. Key: ·····, simplified model; – – – –, Flügge theory; ——, Kennard theory.

part of the standing near field decays to zero, which means that the wavelength of this waves rapidly increases towards infinity. This is accompanied by a large increase in the $\hat{k}_{01}$ wavenumber, which means that its behaviour deviates from that of a longitudinal wave. Similar behaviour can also be seen for the other circumferential modes. For the $n = 0$ mode, only longitudinal and the torsional waves propagate in the pipe wall, implying that the dynamic behaviour of the pipe in this mode is similar to that of a membrane.

The simplified expressions for the flexural wavenumbers $\hat{k}_{11}$ and the standing near field $\hat{k}_{13}$, $\hat{k}_{14}$ wavenumbers of the $n = 1$ mode (equations (23) and (27) respectively) are valid up to frequencies of about $\Omega = 0{\cdot}8$, while that for the near field wavenumber $\hat{k}_{12}$ is consistent up to the ring frequency. At very low frequencies, the $n = 1$ mode (excluding standing near field waves) behaves similarly to the Euler–Bernoulli beam. With increasing frequency it behaves as a Timoshenko beam, and at high frequencies its characteristics change as the real part of the standing near field wave tends to zero. It can be seen that the near field wave cuts on and propagates at about $\Omega = 0{\cdot}6$. This is similar to the behaviour of a Timoshenko beam, and occurs because of rotational inertia and finite shear stiffness. At high frequencies in a Timoshenko beam, two waves propagate, roughly at the shear and longitudinal wave speeds. However, in a pipe the waves speeds differ from these, as can be seen by comparing the wavenumber expressions given in equations (23a, b) and (23c, d).

For the circumferential modes ($n \geqslant 2$), the wavenumbers calculated from the simplified characteristic equations (31), (33) and (37) are consistent with the referenced theories. The small departure is because of the several assumptions made. In the figure, Ω_{co} are the approximate cut-on frequencies. It is difficult to distinguish these frequencies obtained from the simplified and the referenced models because of the slightly different cut-on frequencies. At very low frequencies for $n \geqslant 2$ modes, all waves are standing near field. Just before cut-on, they change to be near field waves, and the frequency range over which the near field wave exists is given by equation (41). It can be seen that this frequency range is greater for the higher modes. Once the wave cuts on and propagates it behaves as a dispersive wave, but at higher frequencies it becomes non-dispersive for a certain frequency range as can be seen by the straight-line regions for $b = 1$ in Figure 4. At higher frequencies still, the $\hat{k}_{n1}$ wavenumber increases as the standing near field wavenumbers decrease as discussed previously. This dependence can clearly be seen by examining equation (37), where the $\hat{k}_{n3}$ and $\hat{k}_{n4}$ wavenumbers appear in the denominator of the expression for $\hat{k}_{n1}$. Evaluation of equation (33) at high frequencies reveals that the near field wavenumber is roughly constant and is of similar magnitude to the circumferential order n.

6. CONCLUSIONS

A simplified characteristic equation of an *in vacuo* pipe has been established using Flügge's shell theory as a basis together with some simplifying assumptions. Using this equation, and collecting the eight wavenumbers into two groups, one large and one small, analytical expressions have been derived for the wavenumbers of the $n = 0$ and 1 modes and the near field waves of the $n \geqslant 2$ modes. This method may also be used for the $n \geqslant 2$ modes but it is only valid just after the wave cuts on, when the flexural wavenumber is still relatively small. Alternative expressions for the flexural wave $n \geqslant 2$ modes have been derived in terms of the cut-on frequency and the wavenumbers of the standing near field wavenumbers.

REFERENCES

1. T. C. LIN and G. W. MORGAN 1956. *Journal of the Acoustical Society of America* **28**, 1165–1176. Wave propagation through fluid contained in a cylindrical, elastic shell.
2. L. CREMER, M. HECKL and E. E. UNGAR 1988 *Structure-Borne Sound*. Berlin, Heidelberg, New York: Springer-Verlag.
3. C. R. FULLER and F. J. FAHY 1982 *Journal of Sound and Vibration* **81**, 501–518. Characteristics of wave propagation and energy distributions in cylindrical elastic shells filled with fluid.

4. M. J. BRENNAN, S. J. ELLIOTT and R. J. PINNINGTON 1993 *Royal Naval Engineering College, Mechanics Group Research Report*, RNEC-RR-93035. Waves in fluid filled pipes.
5. S. FINNVEDEN 1997 *Journal of Sound and Vibration* **208**, 685–703. Simplified equations of motion for the radial–axial vibrations of fluid filled pipes.
6. F. J. FAHY 1985 *Sound and Structural Vibration: Radiation, Transmission and Response*. New York: Academic Press.
7. A. W. LEISSA 1973 *NASA SP*-288. Washington DC: U.S. Government Printing Office. Vibrations of shells.
8. W. FLÜGGE 1962 *Stresses in Shells*. Berlin, Heidelberg, New York: Springer-Verlag.
9. W. VARIYART and M. J. BRENNAN 1999 *ISVR Technical Memorandum No.* 847. Measurement of flexural propagating waves in pipes using shaped PVDF modal sensors.
10. M. HECKL 1962 *Journal of the Acoustical Society of America* **34**, 1553–1557. Vibrations of point-driven cylindrical shells.
11. G. PAVIC 1992 *Journal of Sound and Vibration* **154**, 411–429. Vibroacoustical energy flow through straight pipes.
12. D. J. JOHNS and R. J. ALLWOOD 1968 *Journal of Sound and Vibration* **8**, 147–155. Vibration studies of a ring-stiffened circular cylindrical shell.
13. A. J. YOUNG 1995 *Ph.D. Thesis, University of Adelaide, South Australia*. Active control of vibration in stiffened structures.
14. E. KREYSZIG 1993 *Advanced Engineering Mathematics*. New York: John Wiley & Sons, Inc; seventh edition.
15. B. J. BREVART and C. R. FULLER 1993 *Journal of the Acoustical. Society of America* **94**, 1467–1475. Active control of coupled wave propagation in fluid-filled elastic cylindrical shells.
16. E. H. KENNARD 1953 *Journal of Applied Mechanics* **20**, 33–40. The new approach to shell theory: circular cylinders.

APPENDIX A

In this appendix, non-dimensional wavenumbers of longitudinal, torsional and flexural bending waves of a pipe normalized to its radius are given. These are used to describe the axial wavenumbers of the $n = 0$ and 1 modes of the pipe.

The longitudinal (k_l), torsional (k_s), and flexural (k_b) wavenumbers are, respectively, given by [6]

$$k_l^2 = \rho\omega^2/E, \quad k_s^2 = \rho\omega^2/G, \quad k_b^4 = (\rho A/EI)\omega^2, \tag{A1a–c}$$

where $G = E/2(1 + \nu)$ is the shear modulus, $A = 2\pi ah$ is the cross-sectional area of the pipe, and $I = \pi ah(a^2 + h^2/4)$ is the second moment of area of the pipe. To non-dimensionalize equation (A1), the wavenumbers are normalized to the radius of the pipe, and are given by

$$\hat{k}_l^2 = \frac{\Omega^2}{1 - \nu^2}, \quad \hat{k}_s^2 = \frac{2\Omega^2}{1 - \nu}, \quad \hat{k}_b^4 = \frac{2\Omega^2}{(1 + 3\beta^2)(1 - \nu^2)} \cong 2\hat{k}_l^2, \tag{A2a–c}$$